









Synthesis of Coumarin-Based Organic UV-Visible Probes for the Sensitive Detection and Separation of Metal Ions using Reverse Phase Liquid Chromatography and DFT Modelling

M. Sujatha ¹, K. Mrudula Devi ², Munfis Samir Patel ³, Vladimir Sergeevich Talismanov ⁴, Alimuddin ⁵, Anjoud Harmouzi ⁶, G. Sunita Sundari ⁷, Shiv Alwera ^{8,*}, Ritu Mukherjee ^{9,*}

¹ Department of Chemistry, MES College of Arts, Commerce and Science, Malleswaram, Bangalore-560003, India

² Department of Chemistry, Aditya University, Surampalem, Andhra Pradesh-533437, India

³ Mohammed Al-Mana College for Medical Sciences, Safa-Dammam, Kingdom of Saudi Arabia

⁴ Department of Chemistry, Moscow Institute of Physics and Technology, Dolgoprudny, Moscow Region, 141701, Russian Federation

⁵ Physical Sciences Section (Chemistry), School of Sciences, Maulana Azad National Urdu University, Hyderabad - 500032, Telangana, India

⁶ Organic Chemistry, Catalysis and Environment Laboratory, Sciences Faculty, Ibn Tofail University, BP 133, 14000 Kenitra, Morocco

⁷ Department of Physics, Koneru Lakshmaiah Education Foundation, Vaddeswaram, Guntur-522502, India

⁸ Department of Chemical Science, Indian Institute of Science Education and Research, Mohali, Punjab 140306, India

⁹ Department of Chemistry, Dum Dum Motijheel College, Kolkata-700074, West Bengal, India

* Correspondence: ritu069@gmail.com; Ashiv.kumalwera@gmail.com;

Received: 17.07.2024; Accepted: 11.04.2025; Published: 7.09.2025

Abstract: Two new UV-visible probes (PL1 and PL2) have been prepared by the derivatization of coumarin with 2-hydroxy-1-naphthaldehyde in a Schiff base reaction. Synthesized probes were characterized with spectroscopic techniques. Both probes (PL1 and PL2) showed excellent UV-visible absorption properties, and their λ_{max} was achieved at 315 and 342 nm, respectively. Both probes showed high UV-visible sensitivity for metal ions, specifically Zn^{2+} , Al^{3+} , Fe^{3+} , Mn^{2+} , and Cu^{2+} ions. The ability of the probes was investigated by testing different concentration samples at the nanomolar scale. The effect of various functional groups on detection was investigated in RP-HPLC analysis. The DFT calculations were performed to develop the probes' lowest energy structures and HOMO-LUMO orbitals. The interactions of metal ions with probes (PL1 and PL2) were investigated by developing 3D structures of complexes using DFT.

Keywords: coumarin; naphthalene; derivatives; probes; Schiff base; RP-HPLC.

© 2025 by the authors. This article is an open-access article distributed under the terms and conditions of the Creative Commons Attribution (CC BY) license (<https://creativecommons.org/licenses/by/4.0/>), which permits unrestricted use, distribution, and reproduction in any medium, provided the original work is properly cited. The authors retain copyright of their work, and no permission is required from the authors or the publisher to reuse or distribute this article, as long as proper attribution is given to the original source.

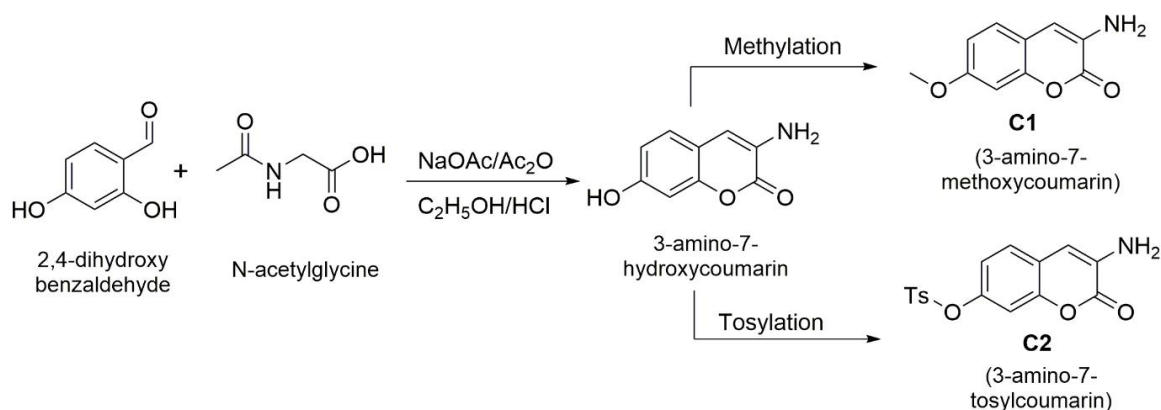
1. Introduction

In recent years, the analysis of metal ions and their concentration in drinking water, food, agricultural soil, rocks, and industrial waste has gained huge attention due to their direct impact on environmental and human health [1,2]. The small amount of heavy metals in dietary is necessary due to their crucial role in biological reactions, e.g. Al^{3+} in lower concentration helps in plant growth, Zn^{2+} is an essential content of blood plasma (12-6 mM) in Humans [3,4],

Fe and Mg metal ions use in preparation of haemoglobin and chlorophyll, respectively, and the Ca^{2+} ion use in formation of skeleton and other metal ions (Ca, Cu, Fe, Mn, Co, Cd) takes part crucial biological catalytic reactions. But metal ions in high amounts cause an adverse effect on humans, e.g. higher concentrations of Al^{3+} (over 3-10 mg according to WHO) cause osteoporosis and Alzheimer's disease [5-8], and higher concentrations of Zn^{2+} cause neurodegenerative disorders [9-11], and the higher concentration of Mg^{2+} and Co^{2+} produce cardiovascular disorder and asthma, lungs disease, thyroid enlargement, dermatitis, and vasodilation [6,7] while higher amount of Fe^{2+} reason for hemochromatosis.

Till now, many detection methods for metal ions from various samples have been developed, including fluorescence spectroscopy, UV-visible spectroscopy, and atomic absorption spectroscopy; among them, the spectroscopic methods are better methods due to low cost and high detection sensitivity for metal ions, but the recovery and separation is not possible with these. All these reported methods are limited to detecting a limited number of metal ions in a single analysis. In many cases, multiple ions disturb the analysis and cause/result in poor accuracy [12,13]. So, to overcome the problem, we are reporting a liquid chromatographic detection method of sensing multiple metal ions in a single run. In this, the metal ions turn into high UV-visible responsive metal complexes with suitable ligands, thus, such a method can be classified as ligand exchange chromatography [14]. Till now, various chromatographic separation methods have been developed and reported for the separation of organic molecules, pharmaceuticals, and chiral compounds [15-18], but the separation of metal ions using liquid chromatography has yet to be reported. In this work, we describe the synthesis of two new coumarin-based UV-visible probes and use them as ligands in reverse phase chromatographic detection and separation of various metal ions. Coumarins are aromatic structures of fused rings that exhibit exceptional luminescence and fluorescence [19,20]. There has been a lot of interest in developing UV-visible and luminescent ligands. Due to the heteroatom (oxygen atom; acts as an electro-donor) in the structure, coumarin-based ligands (probe) have a high binding capacity with various analytes and provide sensitive analyte detection in multiple scenarios [21,22]. Until now, coumarin compounds have been derivatized at an eighth position to create various coumarin-based fluorophores ligands; one such example is the coumarin-nitrobenzene conjugate probe [20]. Ligands based on coumarin have been applied to other areas, such as chromatographic detections, and have been utilized to detect a range of metal cations, including zinc, iron, copper, calcium, magnesium, and others, in various chemical, environmental, clinical, and biological samples [23].

The present report describes the synthesis of two novel Schiff base probes/ligands (PL1 and PL2) prepared on the basic structure of coumarin (Schemes 1, 2, and 3). The structure of coumarin derivatives (C1 and C2) was modified by introducing 2-hydroxy-1-naphthaldehyde in the desired probes, under the Schiff base reaction. In conjugation with naphthalene, the coumarin molecule turns it into a highly UV-visible sensitive probe (PL1 and PL2) for detection and efficiently senses different metal ions in the presence of suitable binding sites. The synthesized probes are used to develop a reverse phase chromatographic detection and separation method for various metal ions from environmental samples. The Develop method was validated for robustness, accuracy, and sensitivity. The stable conformer structures, metal complex, HOMO-LUMO, energy gap optimizations, and elution mechanism were also carried out using DFT simulations. The effect of other participating metal ions on detection was also studied.



Scheme 1. Synthesis of coumarin derivatives C1 and C2.

2. Materials and Methods

Chemical and reagents: The chemicals and solvents used in this study were purchased from Sigma–Aldrich and Avra Chemicals (India).

Instruments and equipment: A Shimadzu HPLC system with a 20 μ L manual injector, a C₁₈ column, and a PDA detector was employed for analysis. The LC solution programme was used to proceed with the results that were obtained. In addition, synthesized products were characterized using an elemental analyzer, an FT-IR instrument, a pH metre, a 500 MHz NMR spectrometer, and a UV-visible spectrometer.

2.1. Experimental.

2.1.1. Synthesis of coumarin derivatives C1 and C2.

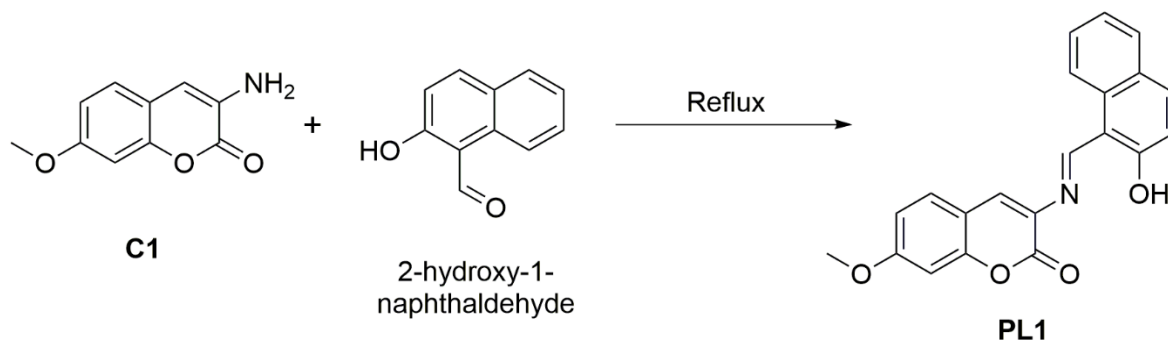
A mixture of N-acetylglycine (1.76 g, 15 mmol), anhydrous sodium acetate (45 mmol), and 2,4-dihydroxy benzaldehyde (2.07 g, 15 mmol) in acetic anhydride (70 mL) was refluxed under stirring for eight hours (Scheme 1). A yellow precipitate was obtained by pouring the reaction mixture into ice (250 mL). Followed by filtration, the yellow solid was refluxed for two hours in a solution of ethanol and concentrated HCl (1:2). The mixture was then poured into ice water (70 mL) and maintained at pH 5~6 by adding 30% NaOH aqueous solution. The solution was then concentrated to 25 mL, and the crude product was precipitated and collected. The obtained compound was then recrystallized in EtOH to give 3-amino-7-hydroxycoumarin [24,25].

The methylation on the hydroxyl group of 3-amino-7-hydroxycoumarin was carried out in an acidic medium, followed by the protection and deprotection of the amino group with fmoc anhydride [26,27] to prepare C1. In contrast, the tosylation of the hydroxyl group of 3-amino-7-hydroxycoumarin was carried out in a basic medium, followed by the protection and deprotection of the amino group with Boc anhydride [28,29] to obtain C2. Both methylation and tosylation reactions yield more than 95% yield.

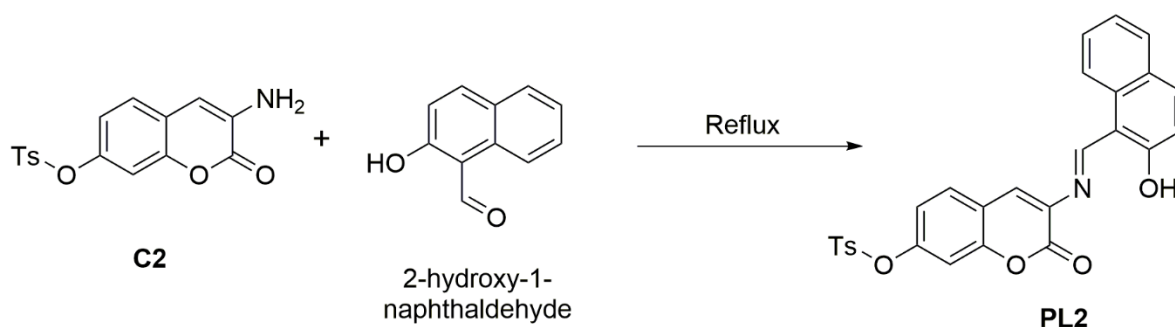
3-amino-7-hydroxycoumarin: yield: 1.58 g, 62%. ¹H NMR (400 MHz, d₆ -DMSO) δ ppm 9.84 (s, 1H), 7.23 (d, J = 8.1 Hz, 1H), 7.04-5.39 (m, 3H), 5.25 (s, 2H); HRMS [C₉H₇NO₃] 178.05 (M+H⁺); Anal. calcd. (found)% for C₉H₇NO₃: C, 61.02 (61.24); H, 3.98 (3.67); N, 7.91 (8.06).

C1: yield: 1.62 g, 95%. ¹H NMR (400 MHz, d₆ -DMSO) δ ppm 7.24 (d, J = 8.1 Hz, 1H), 7.05-5.39 (m, 3H), 5.25 (s, 2H), 3.84 (s, 3H); HRMS [C₁₀H₉NO₃] 192.08 (M+H⁺); Anal. calcd. (found)% for C₁₀H₉NO₃: C, 62.82 (62.56); H, 4.75 (4.21); N, 7.33 (7.58).

C2: yield: 2.84 g, 97%. ¹H NMR (400 MHz, d6 -DMSO) δ 7.82 (d, 2H), 7.36 (d, 2H), 7.34-7.26 (m, 3H), 5.68 (s, 1H), 5.27 (br, 2H), 2.38 (s, 3H); HRMS [C₁₆H₁₃NO₅S] 332.07 (M+H⁺); Anal. calcd. (found)% for C₁₆H₁₃NO₅S: C, 58.01 (57.67); H, 3.95 (4.18); N, 4.23 (4.41); S, 9.68 (8.98).



Scheme 2. Synthesis of coumarin-based probe PL1.



Scheme 3. Synthesis of coumarin-based probe PL2.

2.1.2. Synthesis of coumarin based probes PL1 and PL2.

2-hydroxy-1-naphthaldehyde (0.5 mmol, 0.086 g) in ethanol was mixed with a solution of C1 (0.5 mmol, 0.096 g) in ethanol (Scheme 2). The reaction mixture was then refluxed for twelve hours. Red powder (PL1) was obtained by filtering, washing, and drying the final product in a vacuum chamber three times using ethyl alcohol (3 x 30 mL). A similar synthetic route (Scheme 3) was used to prepare PL2 from C2 [4, 24].

PL1: ¹H NMR (400 MHz; DMSO-d₆): δ (ppm) 15.11 (d, 1H), 9.62 (d, 1H), 8.34 (d, 1H), 8.29 (s, 1H), 7.84 (d, 1H), 7.71 (d, 1H), 7.48 (m, 2H), 7.30 (m, 1H), 6.89 (d, 1H), 6.82 (dd, 1H), 6.75 (d, 1H), 3.84 (s, 3H); IR (KBr): 3474, 3212, 3151, 3083, 2996, 1785, 1700, 1672, 1557, 1493, 1440, 1389, 1295, 1255, 1171, 1035, 949 and 680 cm⁻¹; HRMS [C₂₁H₁₅NO₄] 346.11 (M+H⁺); Anal. calcd. (found)% for C₂₁H₁₅NO₄: C, 73.04 (72.78); H, 4.38 (4.12); N, 4.06 (4.21).

PL2: ¹H NMR (400 MHz; DMSO-d₆): δ (ppm) 15.10 (d, 1H), 9.64 (d, 1H), 8.36 (d, 1H), 8.30 (s, 1H), 7.85 (d, 1H), 7.81 (d, 2H), 7.73 (d, 1H), 7.49 (m, 2H), 7.33-7.24 (m, 3H), 6.91 (d, 1H), 6.84 (dd, 1H), 6.75 (d, 1H), 2.39 (s, 3H). IR (KBr): 3475, 3201, 3159, 1785, 1673, 1555, 11495, 1394, 1286, 1247, 1188, 1140, 961, 856 and 745 cm⁻¹; HRMS [C₂₇H₁₉NO₆S] 486.14 (M+H⁺); Anal. calcd. (found)% for C₂₇H₁₉NO₆S: C, 66.80 (67.08); H, 3.94 (4.06); N, 2.89 (2.71); S, 6.60 (6.18).

Table 1. Sample prepared for RP-HPLC analysis.

S.N	Probe	Metal ion	Sample name	S.N.	Probe	Metal ion	Sample name
1.	PL1	Zn ²⁺	Zn-PL1	7.	PL2	Zn ²⁺	Zn-PL2
2.	PL1	Fe ³⁺	Fe-PL1	8.	PL2	Fe ³⁺	Fe-PL2

S.N	Probe	Metal ion	Sample name	S.N.	Probe	Metal ion	Sample name
3.	PL1	Mn ²⁺	Mn-PL1	9.	PL2	Mn ²⁺	Mn-PL2
4.	PL1	Al ³⁺	Al-PL1	10.	PL2	Al ³⁺	Al-PL2
5.	PL1	Cu ²⁺	Cu-PL1	11.	PL2	Cu ²⁺	Cu-PL2
6.	PL1	All	Mix-PL1	12.	PL2	All	Mix-PL2

2.1.3. Preparation of samples and stock solutions.

1 mM stock solutions of the Al³⁺, Fe³⁺, Zn²⁺, Mn²⁺ and Cu²⁺ were prepared in double distilled water. 1 mM stock solutions of probes (PL1 and PL2) were prepared in acetonitrile. 10 mM TEAP (triethylammonium phosphate) buffer was prepared as reported in the literature [30, 31].

Preparation of samples for RP-HPLC: Sample Zn-PL1 was prepared by mixing 50 μ L solution of stock solution of Zn²⁺ and 60 μ L solution of stock solution PL1, and sonicated for 2 minutes. Similarly, the solution of Fe-PL1, Mn-PL1, Al-PL1, Cu-PL1, Zn-PL2, Fe-PL2, Mn-PL2, Al-PL2 and Cu-PL2 were prepared.

Mix-PL1 and Mix-PL2 samples: To prepare Mix-PL1, 300 μ L solution of the probe PL1 and 50 μ L solution of each metal ion stock solution (total 250 μ L; Al³⁺, Fe³⁺, Zn²⁺, Mn²⁺, and Cu²⁺) was mixed in a vial and sonicated for 2 minutes. Similarly, the Mix-PL2 sample was prepared. The list of the prepared samples for RP-HPLC analysis is given in Table 1.

Each sample was diluted ten times with acetonitrile and filtered before applying it to the RP-HPLC.

Drinking water sample for RP-HPLC: 1000 μ L drinking water mixed with 300 μ L solution of the probe PL1 and 50 μ L solution of each metal ion stock solution (total 250 μ L; Al³⁺, Fe³⁺, Zn²⁺, Mn²⁺, and Cu²⁺) was mixed in a vial and sonicated for 2 minutes. Similarly, the drinking water sample with PL2 was prepared. An aliquot of both samples (50 μ L) was diluted 9 times with acetonitrile and filtered before applying it to the RP-HPLC.

2.1.4. RP-HPLC and conditions for analysis.

The gradient mode was used to separate the prepared complexes of PL1 and PL2 with metal ions (Al³⁺, Fe³⁺, Zn²⁺, Mn²⁺, and Cu²⁺) on RP-HPLC. The eluting phase, buffer (TEAP), and acetonitrile were used in ratios of 20-80%, 30-70%, 40-60%, and 45-55% (in a linear gradient). Filtered and sonicated (degassed) mobile phase used in the RP-HPLC system [32, 33]. Metal complexes were recognised using the PDA detector, and a 1 mL/min flow rate was maintained for the eluting phase.

3. Results and Discussion

Schiff base reactions are reversible and yield aromatic imines as a product by heating aldehyde and aromatic amino groups without any catalyst. Schiff base reactions are prevalent in the preparation of COF, MOF, and organic conjugated ligands/probes that are used as sensors in various fluorophores applications [4,24,25,34,35]. Schiff bases are also used in the preparation of organic dyes, pharmaceuticals, pesticides, cosmetics, and paint pigments, etc [23]. In an intermolecular cyclization reaction of 2,4-dihydroxy benzaldehyde and N-acetyl glycine, the 3-amino-7-hydroxycoumarin was prepared [25], and its hydroxyl group was modified into methoxy and tosyl groups to obtain C1 and C2 derivatives. Two UV-visible probes (PL1 and PL2) were prepared in a Schiff base condensation reaction of 2-hydroxy-1-naphthaldehyde with 3-amino-7-methoxycoumarin (C1) or 3-amino-7-tosylcoumarin (C2) [4,24]. Due to the formation of an imine bond, the conjugation between coumarin and

naphthalene is stabilised. Thus, the enhancement in spectroscopic properties was observed for both probes. The imine bond is significantly less stable and readily reacts with upcoming nucleophiles in an addition reaction and forms amines or amides; also, due to high reactivity, Schiff bases are not stable in the presence of nucleophiles or moderate pH conditions [23,36].

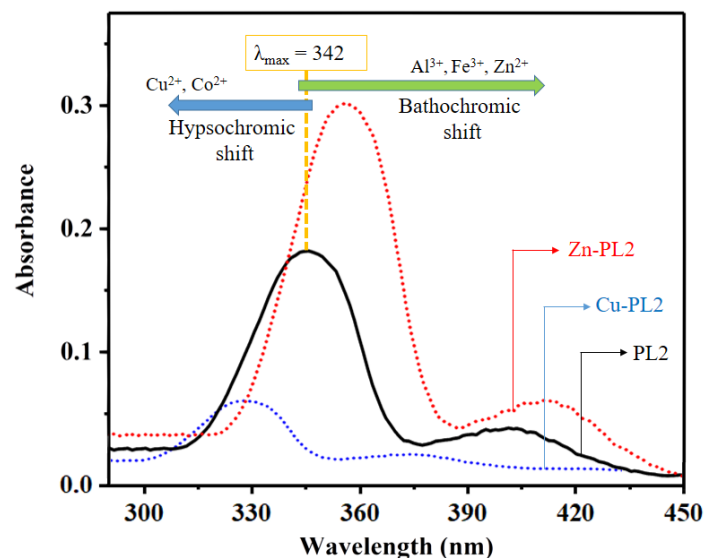


Figure 1. UV-visible spectrum of the PL2 and shifting of λ_{\max} on complex formation with metal ions.

The prepared probes show the keto-enol tautomerism [4, 24] and double bond and hydrogen atom move in between imine and the hydroxyl group of naphthalene, and due to this and free lone pair on nitrogen atom, PL1 and PL2 show excellent binding with several of metal ions (Ag^+ , Al^{3+} , Na^+ , Ni^{2+} , Pb^{2+} , Fe^{3+} , Cd^{2+} , Co^{2+} , Zn^{2+} , Mn^{2+} , Cr^{3+} , Hg^{+2} and Cu^{2+}). Both probes nonselectively bind with different metal ions, and based on different binding energies of complexes with various metal ions, the highest absorption wavelength (λ_{\max}) appeared at different positions in the UV-visible spectrum. Most of the metal ions enhance the absorbance of the probes with bathochromic shift, while Cu^{2+} and Co^{2+} decrease absorption with hypsochromic shift. Among these metal ions, we chose five metal ions (Zn^{2+} , Al^{3+} , Fe^{3+} , Mn^{2+} , and Cu^{2+}) for the separation study. The complex of PL1 and PL2 formed with metal ions' energies and dipole moment was calculated with DFT and provided in Table 3.

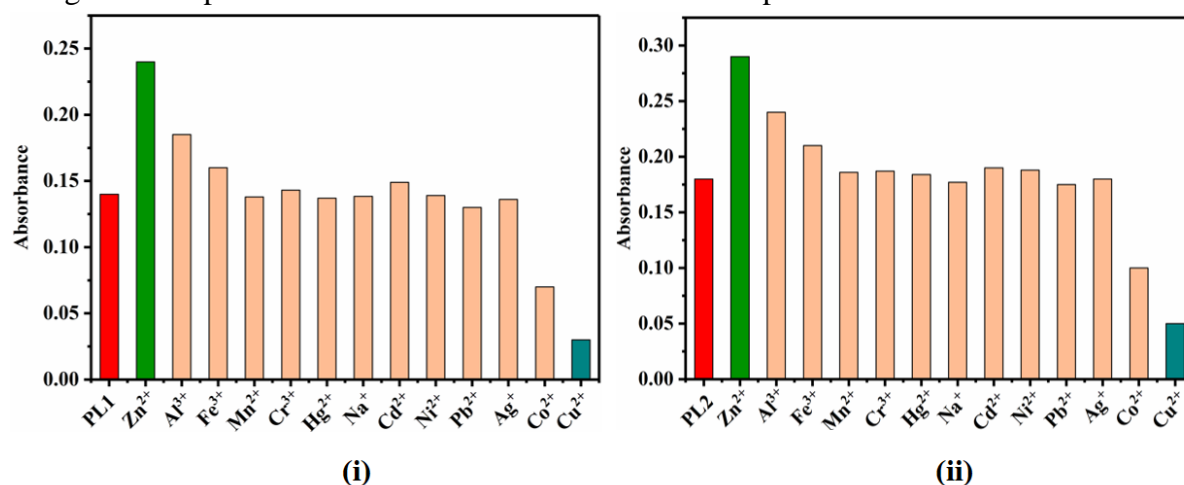


Figure 2. UV-visible response of (i) PL1; (ii) PL2 (5×10^{-5} M) in ACN:H₂O (8.5:1.5%, v/v) upon addition of various metal ions (20×10^{-6} M).

The PL1 and PL2 (probes) both show excellent solubility in polar solvents such as DMSO, DMF, CH₃CN, and CH₃OH in the presence of polar functional groups. The compounds

based on coumarins are known to exhibit intriguing properties related to photoluminescence [4, 24, 37-39]. Therefore, the UV-visible properties of PL1 and PL2 (5×10^{-5} M) were investigated in a combination of acetonitrile (ACN) and buffer (HEPES) (8.5:1.5%, v/v). For the probes PL1 and PL2, the highest absorption was measured at 315 and 342 nm, respectively. The absorption spectrum of PL1 and PL2 was arranged as follows: PL2 > PL1. The primary distinction between the two probes (PL1 and PL2) is the connected functional group (methoxy and tosyl), and it is reasonable to assume that the probe group's electronic effect significantly affects the probes' absorption properties [40, 41].

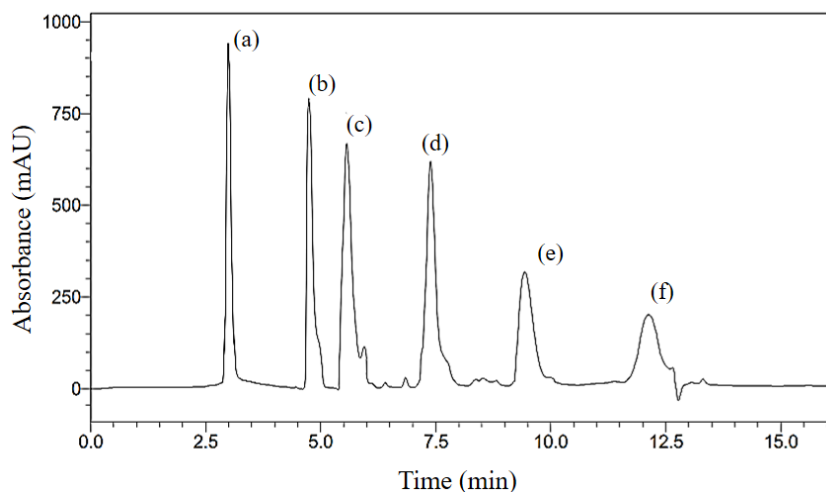


Figure 3. RP-HPLC Chromatogram of the separation of Mix-PL1 (a) Zn-PL1; (b) Al-PL1; (c) Fe-PL1; (d) Mn-PL1; (e) Cu-PL1; (f) PL1.

Due to the presence of appropriate binding sites in the probes (PL1 and PL2), we wished to investigate the chemosensing ability of numerous metal ions such as Ag^+ , Al^{3+} , Na^+ , Ni^{2+} , Pb^{2+} , Fe^{3+} , Cd^{2+} , Co^{2+} , Zn^{2+} , Mn^{2+} , Cr^{3+} , Hg^{2+} , and Cu^{2+} . Many of these metal ions are known to be dangerous environmental pollutants that can be hazardous to health when present in excess [12]. After adding these metal ions, the absorption intensities of PL1 and PL2 solutions significantly alter (Figure 1 displays the UV-visible spectra of PL2 with metal ions as representative). The Co^{2+} and Cu^{2+} ions showed the hypsochromic shift while the remaining metal ions increased the absorption maxima (Figure 1). Also, the Co^{2+} and Cu^{2+} ions quenched the UV-visible spectrum, and the intensity of quenching is directly related to the concentration of these metal ions [12, 13]. (Figure 2 displays the UV-visible absorption response when different metal ions were added to the solution of (i) PL1 and (ii) PL2).

3.1. RP-HPLC analysis.

For the RP-HPLC analysis, only five metal ions (Al^{3+} , Fe^{3+} , Zn^{2+} , Mn^{2+} , and Cu^{2+}) were chosen for study. The sample Mix-PL1 containing different metal complexes with PL1 (Al-PL1, Fe-PL1, Zn-PL1, Mn-PL1, and Cu-PL1) was applied to RP-HPLC separation, and the obtained chromatogram is shown as representative (Figure 3). A clean separation of the different metal complexes (Al-PL1, Fe-PL1, Zn-PL1, Mn-PL1, and Cu-PL1) was achieved on the C_{18} Column of RP-HPLC. The elution order, peak position, and elution time were determined by comparing the chromatograms of individual samples of different metal complexes with PL1. The separation results obtained in the analysis are shown in Table 2. The separation results showed that the complex of Zn-PL1 appears first in the chromatogram with the lowest elution time of 3.02 min. Meanwhile, the Cu-PL1 appears at the end (before the residual peak of PL1) of the chromatogram with an elution time of 9.40 min. Similar results

were achieved for metal complexes prepared with PL2 (analysis of sample Mix-PL2) (chromatographic separation results given in Table 2).

Table 2. Chromatographic elution time and separation data.

S.N.	Mix-PL1	Elution time (min)	Resolution	Mix-PL2	Elution time (min)	Resolution
1.	Zn-PL1	3.02	13.04	Zn-PL2	3.78	13.10
2.	Al-PL1	4.78	9.82	Al-PL2	5.32	10.17
3.	Fe-PL1	5.61	8.18	Fe-PL2	6.18	8.46
4.	Mn-PL1	7.39	5.95	Mn-PL2	8.58	5.46
5.	Cu-PL1	9.42	3.06	Cu-PL2	9.71	3.63
6.	PL1	12.15	-	PL2	12.25	-

A linear gradient mode using TEAP buffer (20%) and acetonitrile (ACN; 80%) was found to be suitable for the eluting phase, which allowed for the separation of all produced metal complexes with probes (PL1 and PL2). The solution's pH (3.5) was kept acidic for optimal separation. The variables such as pH and flow rate of eluting phase, concentration of buffer, and organic modifier were tested for the separation of metal complexes. The organic modifier acetonitrile showed better results when compared to methanol as an eluting phase.

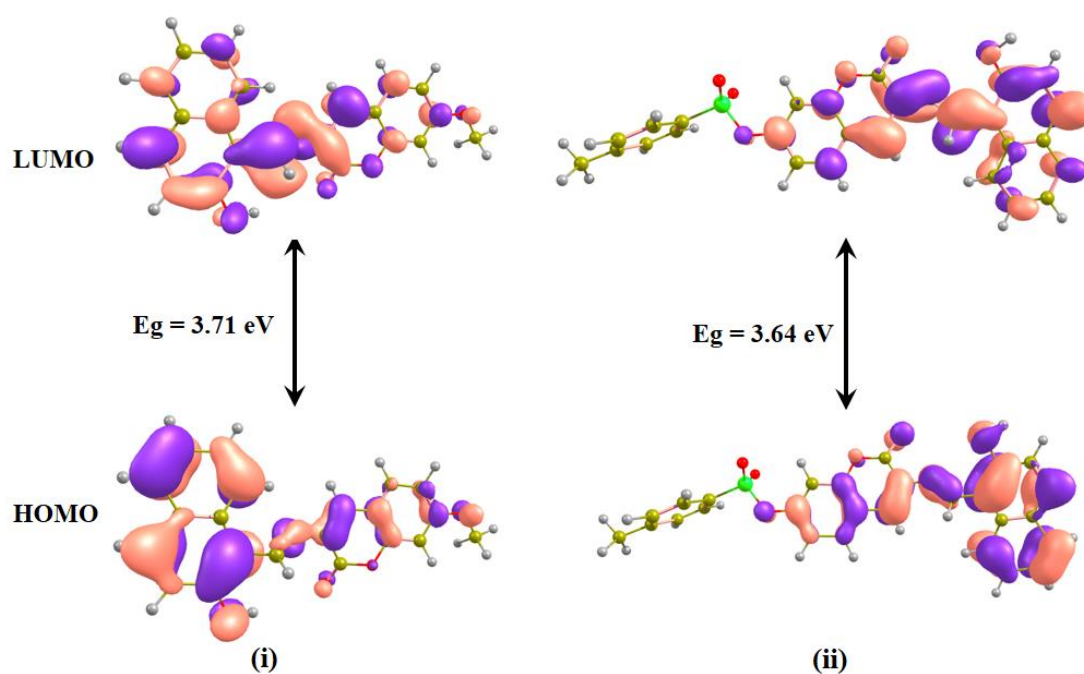


Figure 4. DFT Optimized HOMO-LUMO orbitals diagrams of (i) PL1; (ii) PL2.

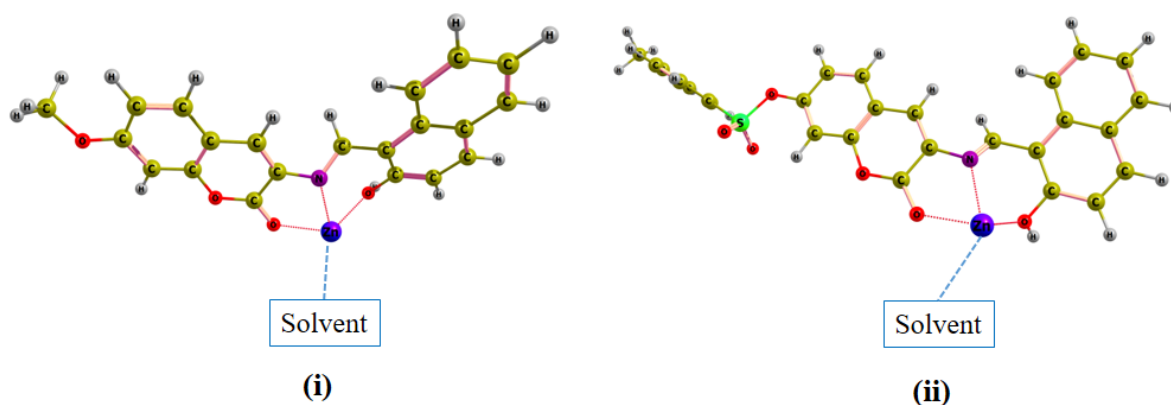


Figure 5. Optimized 3D metal complexes of PL1 and PL2 with Zn^{2+} [(i) Zn-PL1; (ii) zn-PL2].

The peaks obtained during separation were sharp in the case of the acetonitrile organic modifier due to high polarity, low density, and low UV cut-off [16, 42]. The separation results were better when the eluting phase's pH was 3.5, and the flow rate was maintained at 1 mL/min. The high flow rate increased the system pressure, and the low flow rate caused the broadening of the peaks; thus, the RP-HPLC system was run at a 1mL/min flow rate for analysis of metal complexes.

The results [resolution (3.06-13.10) and elution time (3.02-12.25 min)] obtained by the developed method for the separation of metal complexes of Al^{3+} , Fe^{3+} , Zn^{2+} , Mn^{2+} , and Cu^{2+} with PL1 and PL2 are given in Table 2.

Table 3. Metal complexes and optimised dipole moments.

S.N.	Metal complex	Dipole moment (Debye)	S.N.	Metal complex	Dipole moment (Debye)
1.	Zn-PL1	3.02	7.	Zn-PL2	3.78
2.	Al-PL1	4.78	8.	Al-PL2	5.32
3.	Fe-PL1	5.61	9.	Fe-PL2	6.18
4.	Mn-PL1	7.39	10.	Mn-PL2	8.58
5.	Cu-PL1	9.42	11.	Cu-PL2	9.71
6.	PL1	12.15	12.	PL2	12.95

3.2. DFT optimised 3D structures and elution order.

The DFT calculations using Gaussian Software were performed to investigate stable complex structures, elution order, and separation mechanism. In the structure of PL1 and PL2, the difference is the methoxy and tosyl group attached at the 7th Position. In PL2, the tosyl group is vertical with respect to the coumarin moiety; thus, the conjugation between the bonds is restricted, and it acts as an electron-withdrawing group and shifts the λ_{max} (342 nm) to a slightly higher wavelength compared to the λ_{max} (315 nm) of PL1. These results are also supported by the HOMO-LUMO orbitals for PL1 and PL2 (Figure 4). The energy gap between the HOMO-LUMO orbitals of PL1 (3.71 eV) is higher than that of PL2 (3.64 eV), and thus, PL2 has a higher λ_{max} (342 nm) value.

The probe interacts with metal ions with hydroxyl, carbonyl, and nitrogen groups of the imine group and forms metal complexes with each metal ion used in this study, for example, Zn-PL1 and Zn-PL2 shown in Figure 5. The vacant valances of the metal ions were stabilised with solvent molecules (ACN, Water, and TEAP), and these interactions increased the solubility of the metal complexes in the used mobile phase. The planarity of both probes (PL1 and PL2) was increased when they bound with metal ions (as shown in Figure 5); thus, the conjugation between the coumarin and naphthalene was increased and resulted in a higher absorption wavelength compared to the probes (PL1 and PL2).

The separation and elution order of the prepared complexes with PL1 and PL2 depended on the metal complex dipole moment and the number of carbon atoms in the structure. The high carbon number increases the hydrophobic character in the metal complex; thus, these bind strongly with the C_{18} column stationary phase and elute slowly [43-45]. Therefore, the metal complexes prepared with PL1 have a lower elution time compared to metal complexes prepared with PL2. The metal complexes that have high dipole-moment (polarity) solubilised higher in polar mobile phase, thus elute faster compared to the metal complexes those are having lower dipole-moment (Table 3), e.g., the metal complex of Zn-PL1 (elution time 3.02 min; dipole-moment 12.93 Debye) elute first while metal complex Cu-PL1 (elution time 9.42 min; dipole-moment 8.43 Debye) elute in last. The order of elution of metal complexes prepared by PL1 and PL2 is given in Table 2.

3.3. Validation.

The new method was validated for robustness, accuracy, linearity, and repeatability, as reported in previous studies [46–48]. The sample concentration was within the 10-1000 ng/mL range for the validation investigations. Peak area acquired in the RP-HPLC system was used to analyse and quantify the method's recoveries and stabilities. The calculated recovery for metal complexes was found to be more than 99% for inter- and intra-day assays, as representative recovery of the Zn-PL1 was 99.78 and 99.21, respectively, for inter- and intra-day assays. The developed method demonstrated an exceptional level of sensitivity in identifying metal complexes. The lowest value of LOD and LOQ was obtained for Zn-PL2 (0.152 ng/mL and 0.456 ng/mL, respectively). The detailed calculated validation data is given in Table 4.

3.4. Analysis of drinking water.

To do this analysis, a known amount of Al^{3+} , Fe^{3+} , Zn^{2+} , Mn^{2+} , and Cu^{2+} solution was added to drinking water (given in preparation of samples), and then this sample was similarly analyzed on RP-HPLC for detection and separation of different metal ions. The similar separation results and detection sensitivity were achieved for different metal complexes without any disturbance.

Table 4. Calculated method validation data for RP-HPLC separation of metal complexes prepared with PL1 and PL2.

S.N.	Metal complex	Intra-day Assay		Inter-day Assay		LOD (ng mL ⁻¹)	LOQ (ng mL ⁻¹)
		Recovery (%)	RSD (%)	Recovery (%)	RSD (%)		
1.	Zn-PL1	99.78	0.58	99.21	0.62	0.178	0.534
2.	Al-PL1	99.14	1.04	98.76	1.18	0.231	0.693
3.	Fe-PL1	98.65	1.12	98.71	1.43	0.298	0.894
4.	Mn-PL1	97.88	1.38	97.22	1.56	0.372	1.116
5.	Cu-PL1	97.08	1.41	96.84	1.58	1.120	3.360
6.	Zn-PL2	99.52	0.98	99.16	1.07	0.152	0.456
7.	Al-PL2	98.97	1.24	98.34	1.36	0.182	0.547
8.	Fe-PL2	98.26	1.46	97.41	1.71	0.298	0.894
9.	Mn-PL2	97.21	1.68	97.38	1.88	0.312	0.936
10.	Cu-PL2	96.47	1.81	96.08	1.92	0.894	2.682

RSD = relative standard deviation; LOD: limit of detection; LOQ: limit of quantification.

4. Conclusion

Coumarin-based UV-visible probes have been proposed and synthesized in this report. These probes showed great affinity and UV-visible sensitivity for different metal ions and detected them at nanomolar concentrations. The PL2, in the presence of the electron-withdrawing group, shows higher λ_{max} and molar absorbance, thus having better sensitivity than PL1. The effect of the dipole moment, number of carbon atoms, and size of the metal complex on elution order was investigated. Chemical analysis may be utilized with these probes to detect Al^{3+} , Fe^{3+} , Zn^{2+} , Mn^{2+} , and Cu^{2+} metal ion traces in different samples from the environments or industries. Very low values of LOD and LOQs were obtained at 0.152 and 0.456 ng/mL. This method can also be used to analyze Ag^+ , Na^+ , Ni^{2+} , Pb^{2+} , Fe^{2+} , Cd^{2+} , Co^{2+} , Cr^{3+} , and Hg^{2+} . The current method is inexpensive, easy to handle, and shows better sensitivity to other reports using different methods, and the analysis is not affected by the presence of hindering impurities.

Author Contributions

All authors have read and agreed to the published version of the manuscript.

Institutional Review Board Statement

Not applicable

Informed Consent Statement

Not applicable

Data Availability Statement

Data supporting the findings of this study are available upon reasonable request from the corresponding author.

Funding

This research received no external funding.

Acknowledgments

The authors are grateful to Dr. Ritu Mukherjee and Dum Dum Motijheel College, Kolkata, for providing the necessary facilities.

Conflicts of Interest

The authors declare no conflict of interest.

References

1. Malik, L. A.; Bashir, A.; Qureashi, A.; Pandith, A. H. Detection and removal of heavy metal ions: a review. *Environ. Chem. Lett.* **2019**, *17*, 1495-1521, <https://doi.org/10.1007/s10311-019-00891-z>.
2. Moukadiri, H.; Noukrati, H.; Youcef, H. B.; Iraola, I.; Trabadelo, V.; Ouakarroum, A.; Malka, G.; Barroug, A. Impact and toxicity of heavy metals on human health and latest trends in removal process from aquatic media. *Int. J. Environ. Sci. Technol.* **2024**, *21*, 3407-3444, <https://doi.org/10.1007/s13762-023-05275-z>.
3. Tang, L. J.; Cai, M. J.; Zhou, P.; Zhao, J.; Zhong, K. L.; Hou, S.H.; Bian, Y.J. A highly selective and ratiometric fluorescent sensor for relay recognition of zinc(ii) and sulfide ions based on modulation of excited-state intramolecular proton transfer. *RSC Adv.* **2013**, *3*, 16802-16809, <https://doi.org/10.1039/C3RA42931H>.
4. Qin, J.C.; Fan, L.; Li, T.R.; Yang, Z.Y. Recognition of Al³⁺ and Zn²⁺ using a single Schiff-base in aqueous media. *Synth. Met.* **2015**, *199*, 179-186, <https://doi.org/10.1016/j.synthmet.2014.11.030>.
5. Tria, J.; Butler, E. C.V.; Haddad, P.R.; Bowie, A.R. Determination of aluminium in natural water samples. *Anal. Chim. Acta.* **2007**, *588*, 153-165, <https://doi.org/10.1016/j.aca.2007.02.048>.
6. Krejpcio, Z.; Wojciak, R.W. The influence of Al³⁺ ions on pepsin and trypsin activity in vitro. *Pol. J. Environ. Stud.* **2002**, *11*, 251-254.
7. Barcelo, J.; Poschenrieder, C. Fast root growth responses, root exudates, and internal detoxification as clues to the mechanisms of aluminium toxicity and resistance: a review. *Environ. Exp. Bot.* **2002**, *48*, 75-92, [https://doi.org/10.1016/S0098-8472\(02\)00013-8](https://doi.org/10.1016/S0098-8472(02)00013-8).
8. Valeur, B.; Leray, I. Design principles of fluorescent molecular sensors for cation recognition. *Coord. Chem. Rev.* **2000**, *205*, 3-40, [https://doi.org/10.1016/S0010-8545\(00\)00246-0](https://doi.org/10.1016/S0010-8545(00)00246-0).

9. Xu, Z. C.; Baek, K.H.; Kim, H.N.; Cui, J.N.; Qian, X.H.; Spring, D.R.; Shin, J.; Yoon, J. Zn²⁺-triggered amide tautomerization produces a highly Zn²⁺-selective, cell-permeable, and ratiometric fluorescent sensor. *J. Am. Chem. Soc.* **2010**, *132*, 601-610, <https://doi.org/10.1021/ja907334j>.
10. Bhalla, V.; Roopa; Kumar, M. Pentaquinone based probe for nanomolar detection of zinc ions: Chemosensing ensemble as an antioxidant. *Dalton Trans.* **2013**, *42*, 975-980, <https://doi.org/10.1039/C2DT31341C>.
11. Du, P.W.; Lippard, S.J. A highly selective turn-on colorimetric, red fluorescent sensor for detecting mobile zinc in living cells. *Inorg. Chem.* **2010**, *49*, 10753-10755, <https://doi.org/10.1021/ic101569a>.
12. Sehlangia, S.; Nayak, N.; Garg, N.; Pradeep, C.P. Substituent-controlled structural, supramolecular, and cytotoxic properties of a series of 2-styryl-8-nitro and 2-styryl-8-hydroxy quinolines. *ACS Omega* **2022**, *7*, 24838-24850, <https://doi.org/10.1021/acsomega.2c03047>.
13. Sehlangia, S.; Devi, M.; Nayak, N.; Garg, N.; Dhir, A.; Pradeep, C.P. Synthesis, crystal structure and substituent controlled photoluminescence and chemosensing properties of a series of 2,2'-(arylenevinylene)bis-8-hydroxyquinolines. *ChemistrySelect* **2020**, *5*, 5429-5436, <https://doi.org/10.1002/slct.202000674>.
14. Khokhar, F.M.; Jahangir, T.M.; Khuhawar, M.Y.; Khaskheli, M.I.; Khokhar, L.A.; Abro, M.I.; Khaskheli, M.A.; Muqaddisa, P. Analysis of platinum-based anticancer injections cisplatin and carboplatin in blood serum and urine of cancer patients by photometry, fluorometry, liquid chromatography using a Schiff-base as derivatizing reagent. *J. Pharm. Biomed. Anal.* **2024**, *238*, 115808, <https://doi.org/10.1016/j.jpba.2023.115808>.
15. Alwera, S.; Bhushan, R. (R*S*)-Propranolol: enantioseparation by HPLC using newly synthesized (S)-levofloxacin-based reagent, absolute configuration of diastereomers and recovery of native enantiomers by detagging. *Biomed. Chromatogr.* **2016**, *30*, 1223-1233, <https://doi.org/10.1002/bmc.3671>.
16. Alwera, S.; Bhushan, R. Micellar liquid chromatography for enantioseparation of β -adrenolytics using (S)-ketoprofen-based reagents. *J. Liq. Chromatogr. Relat. Technol.* **2017**, *40*, 707-714, <https://doi.org/10.1080/10826076.2017.1348954>.
17. Alwera S.; Bhushan R. RP-HPLC enantioseparation of β -adrenolytics using micellar mobile phase without organic solvents. *Biomed. Chromatogr.* **2017**, *31*, e3983, <https://doi.org/10.1002/bmc.3983>.
18. Alwera, V.; Sehlangia, S.; Alwera, S. Enantioseparation of racemic amino alcohols using green micellar liquid chromatography and confirmation of absolute configuration with elution order. *Sep. Sci. Technol.*, **2021**, *56*, 2278-2286, <https://doi.org/10.1080/01496395.2020.1819826>.
19. Ullah, A.; Bukhari, K.S.; Farooq, F.; Guo, F.H.; Asif, M.; Ullah, A.; Ullah, I. Advances in polybenzocoumarins: synthesis, applications and fluorescent properties. *ChemistrySelect.* **2024**, *9*, e202305170, <https://doi.org/10.1002/slct.202305170>.
20. Sun, X.; Wang, Y.; Zhang, X.; Zhang, S.; Zhang, Z. A new coumarin based chromo-fluorogenic probe for selective recognition of cyanide ions in an aqueous medium. *RSC Adv.* **2015**, *5*, 96905-96910, <https://doi.org/10.1039/C5RA14500G>.
21. Jinhua, X.; Le, W.; Xiqi, S.; João, R. Coumarin-based fluorescent probes for bioimaging: recent applications and developments. *Curr. Org. Chem.* **2021**, *25*, 2142-2154, <https://doi.org/10.2174/1385272825666210728101823>.
22. Pooja Pandey, H.; Aggarwal, S.; Vats, M.; Rawat, V.; Pathak, S.R. Coumarin-based chemosensors for metal ions detection. *Asian J. Org. Chem.* **2022**, *11*, e202200455, <https://doi.org/10.1002/ajoc.202200455>.
23. Cao, D.; Liu, Z.; Verwilt, P.; Koo, S.; Jangjili, P.; Kim, J. S.; Lin, W. Coumarin-based small-molecule fluorescent chemosensors. *Chem. Rev.* **2019**, *119*, 10403-10519, <https://doi.org/10.1021/acs.chemrev.9b00145>.
24. Qin, J.C.; Yang, Z.Y. Fluorescent chemosensor for detection of Zn²⁺ and Cu²⁺ and its application in molecular logic gate. *J. Photochem. Photobiol. A: Chem.* **2016**, *324*, 152-158, <https://doi.org/10.1016/j.jphotochem.2016.03.029>.
25. Long, Y.; Heyang, L.; Lu, S.; Liangliang, L.; Caihong, Z.; Zhen, X. A highly sensitive fluorescence probe for fast thiol-quantification assay of glutathione reductase. *Angew. Chem.* **2009**, *48*, 4034-4037, <https://doi.org/10.1002/anie.200805693>.
26. Kadsanit, N.; Worsawat, P.; Sakonsinsiri, C.; McElroy, C.R.; Macquarrie, D.; Noppawan, P.; Hunt, A.J. Sustainable methods for the carboxymethylation and methylation of ursolic acid with dimethyl carbonate under mild and acidic conditions. *RSC Adv.* **2024**, *14*, 16921-16934, <https://doi.org/10.1039/D4RA02122C>.

27. Gawande, M.B.; Branco, P.S. An efficient and expeditious Fmoc protection of amines and amino acids in aqueous media. *RSC Green Chem.* **2011**, *13*, 3355-3359, <https://doi.org/10.1039/C1GC15868F>.
28. Wu, Y.; Suna, Y.P. Novel chemoselective tosylation of the alcoholic hydroxyl group of syn- α,β -disubstituted β -hydroxy carboxylic acids. *ChemComm* **2005**, 1906-1908, <https://doi.org/10.1039/B416383D>.
29. Ragnarsson, U.; Grehn, L. Dual protection of amino functions involving Boc. *RSC Adv.* **2013**, *3*, 18691-18697, <https://doi.org/10.1039/C3RA42956C>.
30. Alwera, S.; Alwera, V.; Sehlangia, S. An efficient method for the determination of enantiomeric purity of racemic amino acids using micellar chromatography, a green approach. *Biomed. Chromatogr.* **2020**, *34*, e4943, <https://doi.org/10.1002/bmc.4943>.
31. Raffiunnisa, Jaishetty N.; Ganesh, P.; Patel, M.S.; Talismanov, V.S. Synthesis of quinoline-based new chiral derivatizing reagents and its use in the derivatization and enantioseparation of few structurally similar β -blockers using liquid chromatography and structural optimization using DFT. *Asian J. Chem.* **2023**, *35*, 1855-1861, <https://doi.org/10.14233/ajchem.2023.28037>.
32. Shehri, H.S.; Nilugal, K.C.; Joshi, K.K. Synthesis of cyanuric chloride based chiral reagent for RP-HPLC enantioseparation of (RS)-propranolol. *Asian J. Chem.* **2022**, *34*, 376-382, <https://doi.org/10.14233/ajchem.2022.23550>.
33. Alwera V.; Sehlangia S.; Alwera S. A sensitive micellar liquid chromatographic method for the rectification of enantiomers of esmolol, and determination of absolute configuration and elution order. *J. Liq. Chromatogr. Relat. Technol.* **2020**, *43*, 742, <https://doi.org/10.1080/10826076.2020.1798250>.
34. Xu, Q.; Guo, X.; Wang, S.; Feng, Q.; Yan, S.; Yan, Y. Combination of click chemistry and Schiff base reaction: Post-synthesis of covalent organic frameworks as an immobilized metal ion affinity chromatography platform for efficient capture of global phosphopeptides in serum with chronic obstructive pulmonary disease. *J. Sep. Sci.* **2024**, *47*, 2300900, <https://doi.org/10.1002/jssc.202300900>.
35. Kaur, M.; Malik, A.K. Schiff base MOFs and their derivatives for sequestration and degradation of pollutants: present and future. *Environ. Sci. Pollut. Res. Int.* **2023**, *30*, 118801-118829, <https://doi.org/10.1007/s11356-023-30711-5>.
36. Louaileche, T.; Tabti, S.; Djedouani, A.; Shalalin, K.; Alobaid, A.; Maouche, C.; Hannachi, D.; Amamra, S.; Crochet, A.; Evans, H. S.; Warad, I. Synthesis of novel bi-zwitterion Schiff base derivate from 4-hydroxy-2H-pyran-2-one: DFT/HSA-interactions, thermal, physicochemical, TD-DFT and optical activity. *J. Mol. Struct.* **2024**, *1312*, 138351, <https://doi.org/10.1016/j.molstruc.2024.138351>.
37. Khan, D.; Shaily Coumarin-based fluorescent sensors. *Appl. Organomet. Chem.* **2023**, *37*, e7138, <https://doi.org/10.1002/aoc.7138>.
38. Şahin, M.E.; Biryant, F.; Çalışkan, E.; Koran, K. Coumarin-phosphazenes: enhanced photophysical properties from hybrid materials, *Inorg. Chem.* **2024**, *63*, 11006-11020, <https://doi.org/10.1021/acs.inorgchem.4c00379>.
39. Katariya, K.D.; Nakum, K.J.; Soni, R.; Soman, S. S.; Nada, S.; Hagar, M. Coumarin Schiff base derivatives: Synthesis, mesomorphic properties, photophysical properties and DFT studies. *J. Mol. Struct.* **2023**, *1278*, 134934, <https://doi.org/10.1016/j.molstruc.2023.134934>.
40. Patil, P.; Patil, A.; Pradeep, C.; Sahoo, S.K.; Patil, U. A new phthalimide based chemosensor for selective spectrophotometric detection of Cu(II) from aqueous medium, *Spectrochim. Acta A Mol. Biomol. Spectrosc.* **2019**, *220*, 117129, <https://doi.org/10.1016/j.saa.2019.05.034>.
41. Sehlangia, S.; Sharma, S.; Sharma, S.K.; Pradeep, C.P. 2,2'-(Arylene-divinylene)bis-8-hydroxyquinolines exhibiting aromatic π - π stacking interactions as solution-processable p-type organic semiconductors for high-performance organic field effect transistors. *Mater. Adv.* **2021**, *2*, 4643-4651, <https://doi.org/10.1039/D1MA00215E>.
42. Alwera, S.; Bhushan, R. Liquid chromatographic enantioseparation of three beta-adrenolytics using new derivatizing reagents synthesized from (S)-ketoprofen and confirmation of configuration of diastereomers. *Biomed. Chromatogr.* **2016**, *30*, 1772-1781, <https://doi.org/10.1002/bmc.3752>.
43. Ahmed, T.I.; Talismanov, V.S.; Jaishetty, N. Pre-column Derivatization and Separation of Diastereomeric Derivatives of Racemic Mexiletine and Confirmation of Elution Order and Molecular Configuration. *Asian J. Chem.* **2022**, *34*, 1212-1219, <https://doi.org/10.14233/ajchem.2022.23706>.
44. Shehri, H.S.; Patel, M.S.; Talismanov, V.S.; Macadangang, J.R. Photocatalytic degradation of rhodamine B dye by using Tin-doped CeO₂-Fe₂O₃ nanocomposite. *Asian J. Chem.* **2022**, *34*, 673-680, <https://doi.org/10.14233/ajchem.2022.23578>.

45. Kanyó, T.; Kónya, Z.; Kukovecz, Á.; Berger, F.; Dékány, I.; Kiricsi I. Quantitative characterization of hydrophilic–hydrophobic properties of MWNTs surfaces. *Langmuir* **2004**, *20*, 1656-1661, <https://doi.org/10.1021/la035702r>.
46. Alwera, V.; Sehlangia, S.; Alwera, S. Micellar liquid chromatographic green enantioseparation of racemic amino alcohols and determination of elution order. *Biomed. Chromatogr.* **2020**, *34*, e4954, <https://doi.org/10.1002/bmc.4954>.
47. Alwera, S. In situ derivatization of (*RS*)-mexiletine and enantioseparation using micellar liquid chromatography: a green approach, *ACS Sustainable Chem. Eng.* **2018**, *6*, 11653-11661, <https://doi.org/10.1021/acssuschemeng.8b01869>.
48. Guidance for Industry: Q2B Validation of Analytical Procedures: Methodology. ICH: **1996**.

Publisher's Note & Disclaimer

The statements, opinions, and data presented in this publication are solely those of the individual author(s) and contributor(s) and do not necessarily reflect the views of the publisher and/or the editor(s). The publisher and/or the editor(s) disclaim any responsibility for the accuracy, completeness, or reliability of the content. Neither the publisher nor the editor(s) assume any legal liability for any errors, omissions, or consequences arising from the use of the information presented in this publication. Furthermore, the publisher and/or the editor(s) disclaim any liability for any injury, damage, or loss to persons or property that may result from the use of any ideas, methods, instructions, or products mentioned in the content. Readers are encouraged to independently verify any information before relying on it, and the publisher assumes no responsibility for any consequences arising from the use of materials contained in this publication.